

## Deep-learning based image reconstruction for MRI-guided near-infrared spectral tomography: supplement

JINCHAO FENG,<sup>1,2,3</sup> WANLONG ZHANG,<sup>1,2</sup> ZHE LI,<sup>1,2,5</sup>  KEBIN JIA,<sup>1,2</sup> SHUDONG JIANG,<sup>3,6</sup>  HAMID DEGHANI,<sup>4</sup>  BRIAN W. POGUE,<sup>3</sup>  AND KEITH D. PAULSEN<sup>3,7</sup>

<sup>1</sup>Beijing Key Laboratory of Computational Intelligence and Intelligent System, Faculty of Information Technology, Beijing University of Technology, Beijing 100124, China

<sup>2</sup>Beijing Laboratory of Advanced Information Networks, Beijing 100124, China

<sup>3</sup>Thayer School of Engineering, Dartmouth College, Hanover, New Hampshire 03755, USA

<sup>4</sup>School of Computer Science, University of Birmingham, Birmingham, B15 2TT, UK

<sup>5</sup>e-mail: lizhe1023@bjut.edu.cn

<sup>6</sup>e-mail: shudong.jiang@dartmouth.edu

<sup>7</sup>e-mail: keith.d.paulsen@dartmouth.edu

---

This supplement published with Optica Publishing Group on 24 February 2022 by The Authors under the terms of the [Creative Commons Attribution 4.0 License](https://creativecommons.org/licenses/by/4.0/) in the format provided by the authors and unedited. Further distribution of this work must maintain attribution to the author(s) and the published article's title, journal citation, and DOI.

Supplement DOI: <https://doi.org/10.6084/m9.figshare.18662870>

Parent Article DOI: <https://doi.org/10.1364/OPTICA.446576>

# Deep Learning based Reconstruction of MRI Guided Near Infrared Spectral Tomography Avoids the Limitations of Forward Diffuse Modeling: supplemental document

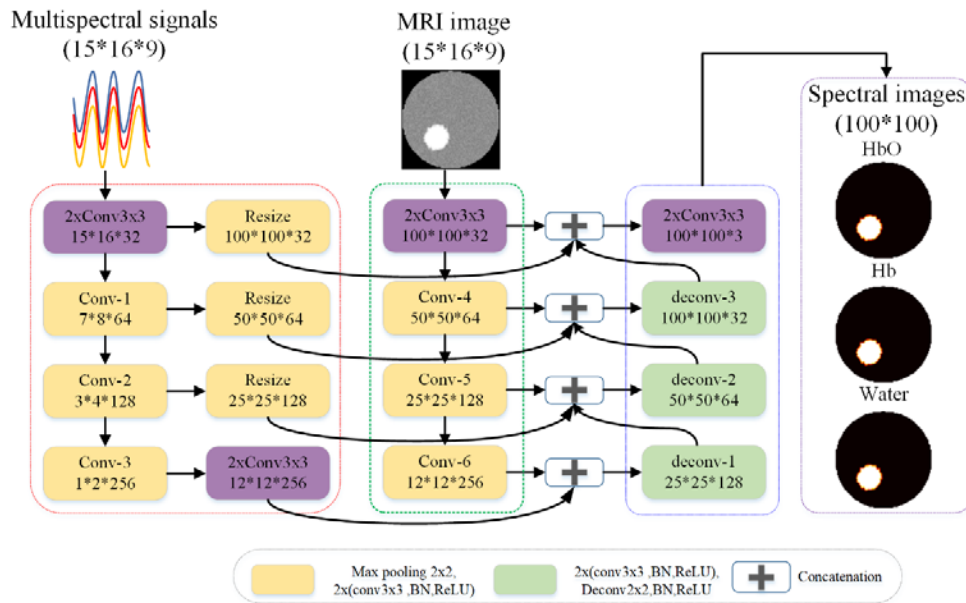


Fig. S1. Architecture of the Y-Net used in this study. All operations are accompanied by a batch-normalization (BN) and ReLU.

Table S1. Chromophore properties used for generating datasets.

Chromophore	Background	Inclusion	Contrast
HbO [ $\mu\text{M}$ ]	15	18	1.20
	16	24	1.50
	17.5	28	1.60
Hb [ $\mu\text{M}$ ]	7.5	9	1.20
	8	10	1.25
	8.5	13.6	1.6
Water [%]	30%	45%	1.50
	50%	85%	1.70
	40%	80%	2.00

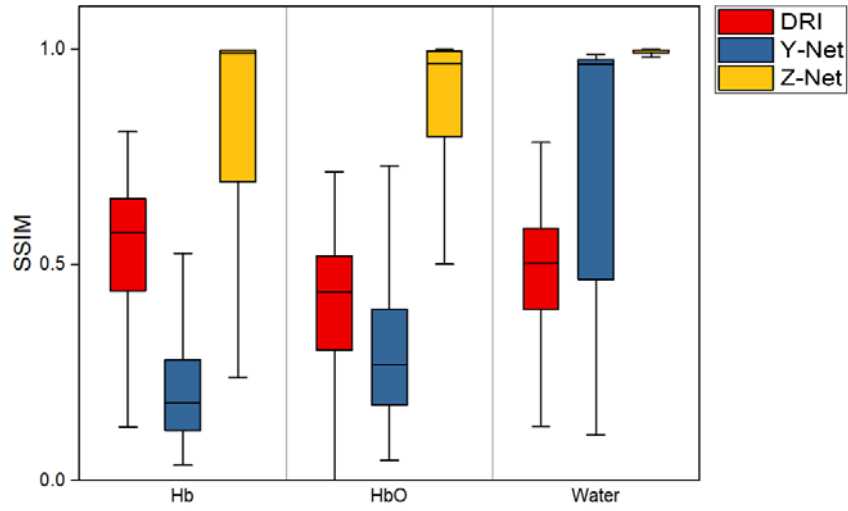


Fig. S2. Statistical results for three algorithms for SSIM.

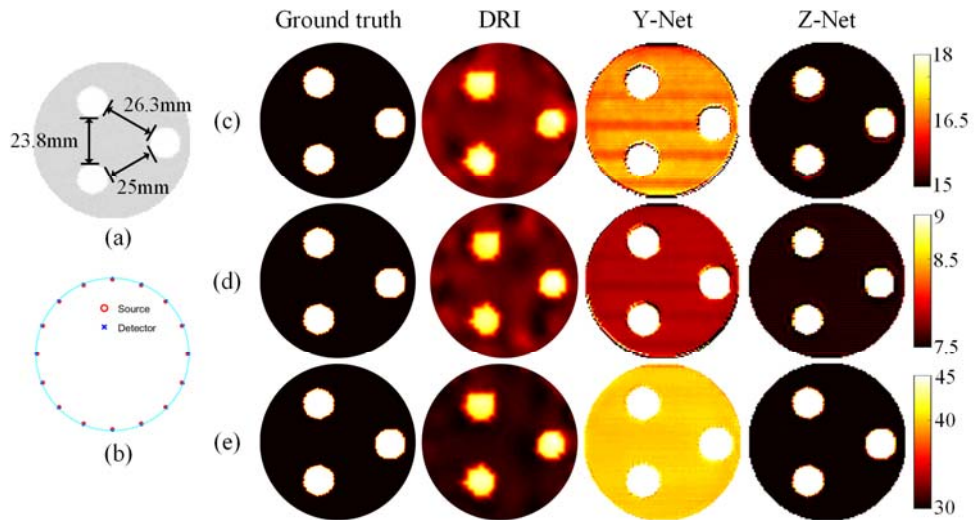


Fig. S3. Reconstructed images of HbO, Hb, and water in the case of three inclusions. (a) MRI images, (b) source/detector positions around the phantom, (c)-(e) true and reconstructed images of HbO, Hb, and water, respectively.

Table S2. Quantitative results for different methods in the case of three inclusions.

Evaluation metric	Algorithm	HbO	Hb	Water
MSE	DRI	0.27	0.07	6.7
	Y-Net	2.57	0.12	9.33
	Z-Net	0.02	0.01	0.02
PSNR (dB)	DRI	12.6	11.7	13.8
	Y-Net	13.5	20.5	18.3
	Z-Net	39.3	36.1	44.8
SSIM	DRI	0.49	0.62	0.62
	Y-Net	0.14	0.67	0.52
	Z-Net	0.95	0.96	0.96

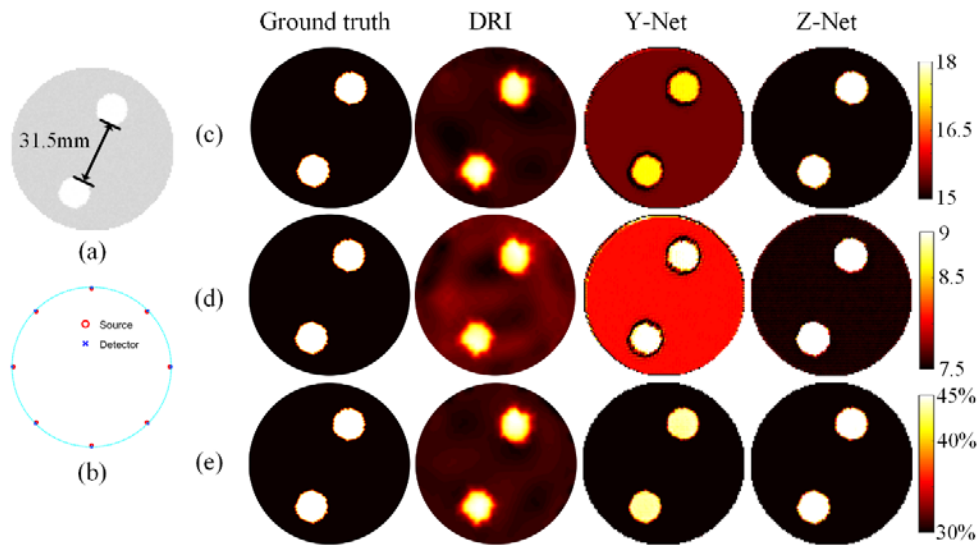


Fig. S4. Reconstructed images with 8 source-detector pairs. (a) MRI image, (b) source/detector positions around the phantom, (c)-(e) are reconstructed images of HbO, Hb, and water, respectively.

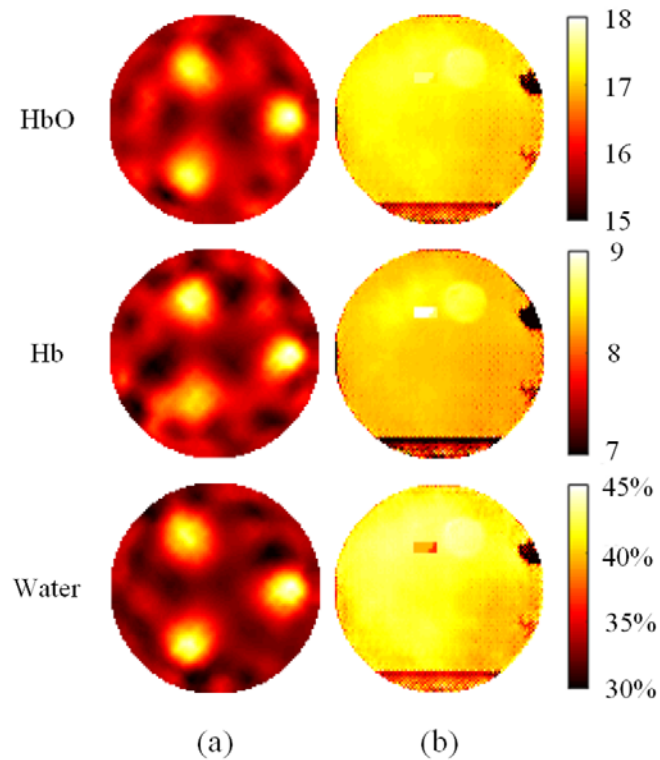


Fig. S5. Reconstructed images without MRI guidance in the case of three phantom inclusions. (a) Images recovered with a traditional reconstruction algorithm [20]; (b) Images reconstructed with the Z-Net architecture but without MRI guidance.